LUMA-GIS Thesis nr 7

Near real-time mapping of floodwater mosquito breeding sites using aerial photographs

Martina Schäfer

2010
Dept. of Earth and Ecosystem Sciences
Division of Physical Geography and Ecosystem Analysis
Centre for Geographical Information Systems
Lund University
Sölvegatan 12
S-223 62 Lund
Sweden

A Master thesis presented to

Department of Physical Geography and Ecosystem Analysis

Centre for Geographical Information Systems

of

LUND
UNIVERSITY

by

Martina Schäfer

in partial fulfilment of the requirements

for the degree of Master in Geographical Information Science

Supervisors:

Ulrik Mårtensson, Lund University

Summary

Floodwater mosquitoes occur in temporary flooded areas and can cause tremendous nuisance in the near and far surroundings. In the Nedre Dalälven region in Central Sweden, mosquito control is based on application of the biological larvicide *Bacillus thuringiensis israelensis (BTI)* by helicopter. Precise mapping of the floodwater mosquito breeding sites, a prerequisite for successful BTI treatments, is complicated by high and dense vegetation, inaccessibility, and time constraints. The aim of this study is to develop a method for quick and easy delineation of flooded areas to direct mosquito control treatments.

Aerial photographs taken from helicopter were used for georeferencing (including test of two flight heights, different helicopter types and camera parameters) and for flood delineation (applying visual interpretation and unsupervised classification) during spring (May) and summer (August) conditions. The study was performed in the Norrån catchment west of the town of Österfärnebo during 2007 and 2008. All photographs were taken with a hand-held Pentax 10D digital camera and a 16-45 mm lens.

The hand-held digital camera gave vertical images of sufficient quality for georeferencing in a GIS. Images taken from a flight height of 600 m and with wide-angle lens could easily be orientated and georeferenced. The best helicopter type for photography was the Eurocopter AS 350 B3 (also used for mosquito control).

Flood delineation by visual interpretation, using image enhancement, provided accurate information about location and extent of flooded areas in May with low and sparse vegetation. However, in August with high and dense vegetation, the vegetated flooded areas were difficult to distinguish from vegetated non-flooded areas. Also, one of the study areas had no sharp edge between flooded and dry areas but rather a transition zone. Similarly, unsupervised classification showed better results (based on accuracy assessments) for images from May than from August.

Finally, the assumed flooded area to be included for mosquito control was digitized based on enhanced images and classification results. In comparison to the actual mosquito control polygons, the boundaries digitized from classifications were most similar. Areas for mosquito control treatments can include small dry parts in order to keep rather straight borderlines which makes helicopter flight movements less time-consuming.

In conclusion, the best method was taking photographs in 8-bit jpg, georeferencing them for use in GIS, and to use a combination of unsupervised classification and on-screen digitizing of the boundaries of flooded areas. This method was used in an inaccessible area during an actual mosquito control treatment in 2009 and provided valuable information about slightly larger flooded areas than initially assumed. Further improvements might be achieved by using the near-infrared spectrum for water detection, and using fuzzy classification in areas with transition zones between flooded and dry sites.

Contents

1 Introduction

1.1 Floodwater mosquitoes

Floodwater mosquitoes such as *Aedes sticticus* and *Aedes vexans* develop in temporary flooded areas along rivers and lakes and can cause tremendous nuisance in the near and far surroundings (Becker et al. 2003). In Sweden, mass emergence of *Aedes sticticus* is well-documented from the River Dalälven flood plains in Central Sweden (Schäfer et al. 2008). In this region, enormous numbers of mosquitoes have been reported with up to 62,100 individuals in one trap and night. In comparison, the maximum number of mosquitoes per trap and night in northern Sweden at Allavaara accounted for 2600 individuals. During recent years, nuisance caused by floodwater mosquito species has been observed at other places in Central and Southern Sweden. The geographic distribution of *Aedes sticticus* has increased, and further expansion due to climate change is predicted (Schäfer and Lundström 2009).

Floodwater mosquito species lay their eggs on moist soil that is subsequently flooded when the water level rises. They have four larval stages followed by the pupal stage before the adults emerge. The larval development is temperature-dependent. Hatching of *Aedes sticticus* larvae from eggs requires water temperature of at least 8°C. The optimum temperature for larval development is approximately 25°C, resulting in development time of 6-8 days from hatching of larvae to emergence of adults (Becker et al. 2003). Females of both *Aedes sticticus* and *Aedes vexans* are known for their long-range dispersal ability and have been shown to disperse at least 10 km from larval sites (Brust 1980).

The larval habitats of floodwater mosquitoes include a variety of shallow temporary water in both open and forested environments. The largest inundation areas are found in the floodplains adjacent to large rivers (e.g. River Dalälven in Sweden, River Rhine in Germany) where the extent of the flooding is dependent on water level of the river. Other inundation wetlands are influenced by small creeks and local rainfall. The temporary wetlands can be situated in open environments, e.g. wet meadow, marsh and abandoned farmland, as well as in forested environments, e.g. alder swamp. The wetlands vegetation is shaped by the regularity and duration of the flooding events. During the spring flood, vegetation is sparse, while at late summer floods, vegetation (mainly grassy vegetation) can be very dense.

1.2. Mosquito control

After a massive mosquito outbreak in the lowlands of the River Dalälven in 2000, the project Biological Mosquito Control was started with the aim to reduce mosquito nuisance in human settlements in and close to the floodplains.

Since 2002, mosquito control measures in the temporary flooded areas are based on application of the biological larvicide *Bacillus thuringiensis israelensis* (BTI) by helicopter (Schäfer and Lundström 2006). Protein crystals produced by the bacteria are the active ingredient of BTI products. These crystals have to be digested by the mosquito larvae to be transformed to active toxins killing the larvae. BTI is an environmentally friendly control agent with high selectivity against larvae of a few families within the suborder Nematocera of the order Diptera. The family mosquitoes (Culicidae) are the most sensitive organisms, requiring the lowest dosage. Early instars are more susceptible than older instars, while pupae no longer feed and thus are not susceptible to BTI at all.

The working mechanisms of BTI lead to some requirements for effective mosquito control. The protein crystals are not persistent and get easily destroyed by sunlight. In the water, it can be

efficient for up to 48 hours (http://extoxnet.orst.edu/pips/bacillus.htm). Thus, control measurements have to be conducted after each flood event leading to hatching of mosquito larvae. Also, treatments have to be implemented quickly after hatching of larvae. During summer, the time window for efficient control measures is approximately one week after hatching.

Precise mapping of the floodwater mosquito breeding sites is a prerequisite for successful BTI treatments. Within Biological Mosquito Control in the River Dalälven floodplains, we combine GPS field measurements, elevation data, and data from previous treatments in a GIS (Schäfer and Lundström 2006). Field measurements are done by identifying the boundary of a flooded area and taking several GPS measurements along this boundary. These measurements are then transferred to a GIS and overlayed on a digital elevation model (DEM). The DEM is derived from air-borne laserscanning with high precision. Based on the elevation data, a threshold elevation for the flood is defined and employed in a query of the elevation model. This results in a raster of the flooded area. With this information and information from previous treatments at similar flood events, the area to be treated by helicopter is digitized on screen.

Nevertheless, complex situations can occur at floodings caused by heavy rain during summer. Rainwater is kept in shallow spots, providing additional breeding sites at higher elevation than the areas flooded by the river. Furthermore, high and dense vegetation during summer is complicating detection of flooded areas. Some inaccessible areas can be problematic under time constraints. Therefore, remote sensing using aerial photographs is suggested as a method to help mapping such areas.

1.3 Aim

The aim of this project is to develop a method for quick and easy delineation of temporary flooded areas to direct mosquito control treatments in inaccessible areas. Aerial photographs taken with a hand-held camera from helicopter are tested for their potential with regard to georeferencing and flood delineation. The specific objectives of this study include evaluation of:

- appropriate camera parameters and image formats
- flight heights
- helicopter types
- flood delineation under spring (low and sparse vegetation) and summer conditions (high and dense vegetation)
- flood delineation with visual interpretation and unsupervised classification
- digitized boundaries for mosquito control areas based on flood delineation methods

2 Methods

2.1 Study Area

As a general study area, the Norrån-catchment area west of the town of Österfärnebo, Nedre Dalälven region in Central Sweden, was chosen (Figure 2.1.1). The river Norrån is connected to Lake Färnebofjärden, a part of the River Dalälven, by Lake Fängsjön. Floods usually occur after melting of snow in spring and/or after heavy summer rains. Water level of the River Dalälven is monitored at the Ista automatic hydrological station, located in Lake Färnebofjärden (Figure 2.1.1). The water level in the Norrån system is normally about 20 cm higher than measured at Ista.

Four areas in the catchment were selected (Figure 2.1.2). Area A is located in the northern forested part of the catchment. Area B is situated in the eastern part consisting of mixed open grassy and bushy vegetation, representing a very inaccessible area. During actual floods, time constraints required easily accessible areas, thus two areas, C and D, were chosen that are located close to roads. Area C is located in the north-western part with mainly herbaceous vegetation. Area D, situated in the western part, consists of herbaceous vegetation with large stands of willows.

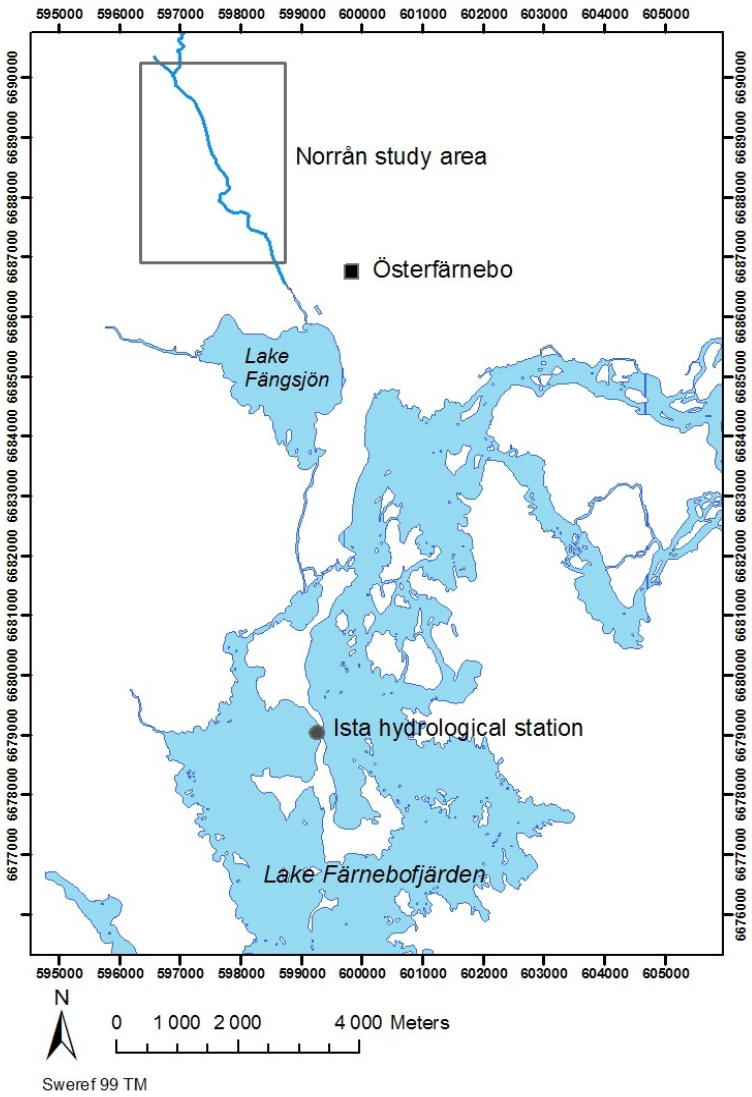

Figure 2.1.1. Location of the Norrån study area for aerial photographs, and the hydrological station Ista in Lake Färnebofjärden, Central Sweden.

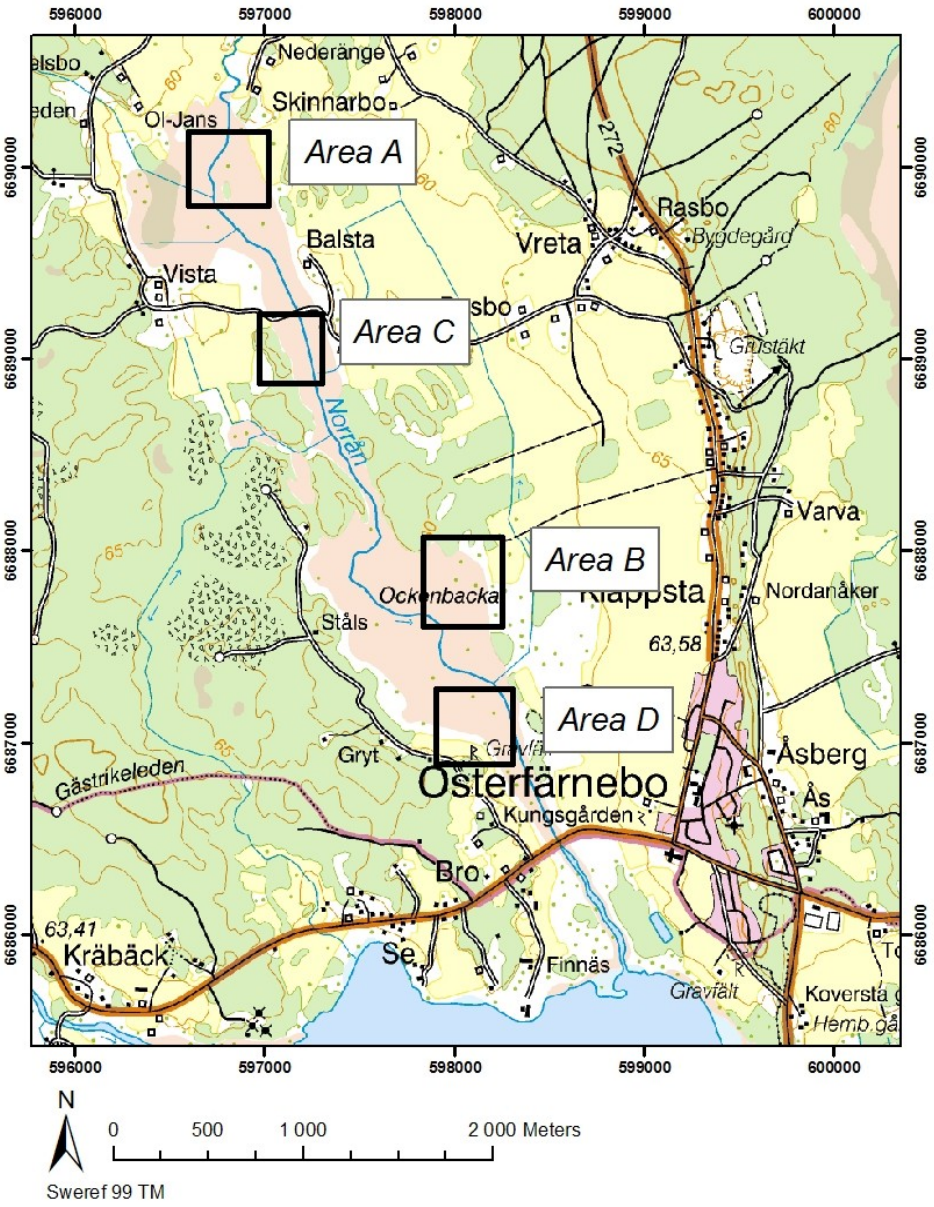

Figure 2.1.2. Location of study areas for aerial photographs of temporary flooded areas in the Norrån area near Österfärnebo, Central Sweden.

Two flood situations in 2008 were included in this study. In May 2008, snow melt in combination with rain caused very high water levels with a maximum of 56.99 m a.s.l. (RH70) at the automatic hydrological station at Ista, Färnebofjärden, on May 11 (Figure 2.1.3). On the day of photographing, May 22, the water level had decreased to 56.52 m a.s.l. (corresponding to a water level of 56.75 m a.s.l. in the Norrån system based on GPS measurements). The water level decreased rapidly from the maximum level but stayed rather high during the rest of May. In the middle of August, water levels increased again due to continuous rainfall. Maximum water level at Ista was 56.39 m a.s.l. on August 23, which would indicate a water level of 56.59 for the Norrån system. However, GPS measurements for mosquito control showed that the local water level in the Norrån system was 56.90 m a.s.l., due to the combined effect of increased water flow in the Dalälven and heavy local rain. This caused a flood situation where the edge of the flooded area could be hard to define due to numerous isolated puddles that could be as small as a couple of dm in diameter, in particular in study areas B and D. These shallow puddles provide excellent breeding sites for floodwater mosquitoes and thus need to be included in the areas for mosquito control treatments.

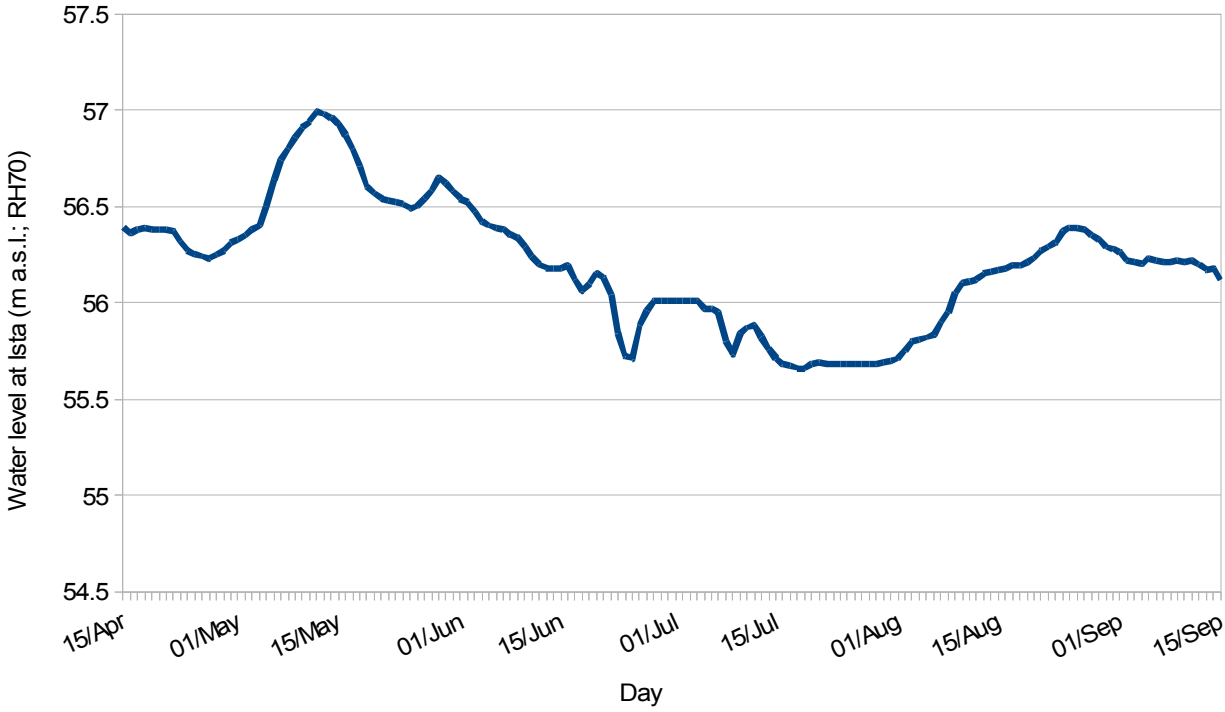

Figure 2.1.3. Water level fluctuations at the Ista automatic hydrological station, Färnebofjärden, Central Sweden, from April 15 to September 15 , 2008.

2.2 Photographing

All photographs were taken with a Pentax 10D digital camera using a 16-45 mm lens. The CCD covers 23.5 mm x 15.7 mm with 3872 x 2592 pixels at highest resolution. The camera has a shake reduction system enabling sharp blur-free images under demanding conditions by a compensation effect equivalent to two to four shutter-speed steps. Pictures can be saved in format jpg or raw with possibility for further processing in the software Pentax Photo Laboratory. Pictures taken in raw-format need to be saved as jpg or tiff files prior to importing to GIS software. In 2007 and in May 2008 all pictures were taken in jpg-format, while in August 2008 pictures were taken in raw-format, then saved as 8 bit jpg (as previously), 16 bit tiff, and in both formats but preceded by "full auto processing" in Pentax Photo Laboratory (Table 2.2.2). Full auto processing of raw-format means that the images are processed using the shootings settings.

Three different helicopter types were employed, Eurocopter EC 120, Eurocopter AS 350 B3 (also used for mosquito control), and Bell 206 Jet Ranger. In the Eurocopter EC 120 and the Bell 206 Jet Ranger, the window on the front passenger seat was opened and enabled holding out the camera and straight downwards. With the Eurocopter AS350 B3, the back door was opened and the photographer was secured with a harness to be able to lean out and hold the camera vertically downwards. (Figures 2.2.1 and 2.2.2).

In April 2007, two flight heights (300 m and 600 m) were tested in areas A and B, based on parameters calculated following Falkner and Morgan (2002) (Table 2.2.1). Using the camera's wide angle from 600 m height almost tripled the ground area covered on the image. In May 2007, May 2008 and August 2008, images were taken from 600 m height only since this allowed for larger coverage. Data on the images selected for further analysis is summarized in Table 2.2.2. In 2007, images were taken with the aim of testing flight and camera parameters and georeferencing of images. In 2008, photographing was conducted during flooded periods with the aim of testing methods for flood delineation.

Table 2.2.1. Calculated parameters for aerial photographs taken with Pentax 10D digital camera.

Focal length (mm)	flight height (m)	Scale	size covered on ground (m x m)	pixel size (m)
45	300	1:6667	157 x 105	0.04
45	600	1:13333	313 x 209	0.08
16	600	1:37500	881 x 589	0.23

Figure 2.2.1. Preparing for taking aerial photographs from Eurocopter AS 350 B3 by flying with open back door and secured with harness. Pilot Michael Elmeskog. (Photograph by Tanja Zaubek)

Figure 2.2.2. Taking photographs from Eurocopter AS 350 B3, flying with open back door. (Photograph by Jan Lundström)

Table 2.2.2. Summary of parameters for selected aerial photographs of flooded temporary areas in the River Dalälven floodplains in 2007 and 2008.

Year	Date and time	Helicopter	Area	Flight height (m)	Focal length (mm)	format	Images	Main analysis
2007	April 10; 11.00-11.15	Eurocopter EC120	area A	300, 600	45	8 bit jpg	April07_areaA	Georeferencing
			area A	600	16		April07_areaA_wa	
			area B	300, 600	45		April07_areaB	
			area B	600	16		April07_areaB_wa	
2007	May 23; 17.30-17.45	Bell 206 Jet Ranger	area B	600	16	8 bit jpg	May07_areaB	Georeferencing
2008	May 22; 9.45-9.55	Eurocopter EC120	area B	600	16	8 bit jpg	May08_areaB	Flood delineation
			area C	600	16		May08_areaC	
2008	August 22; 10.00-10.15	Eurocopter AS 350 B3	area C	600	16	raw → 8 bit jpg	Aug08_areaC_1	Flood delineation
			area C	600	16	raw → full auto processing, 8 bit jpg	Aug08_areaC_2	
			area C	600	16	raw → 16 bit tiff	Aug08_areaC_3	
			area C	600	16	raw → full auto processing, 16 bit tiff	Aug08_areaC_4	
			area D	600	16	raw → 8 bit jpg	Aug08_areaD_1	
			area D	600	16	raw → full auto processing, 8 bit jpg	Aug08_areaD_2	
			area D	600	16	raw → 16 bit tiff	Aug08_areaD_3	
			area D	600	16	raw → full auto processing, 16 bit tiff	Aug08_areaD_4	

2.3 Georeferencing

White Styrofoam squares (56.8 x 56.8 cm) were used as markings for georeferencing. The position of these markings was measured using a DGPS (Ashtech G12 with a TDS Recon PDA). Five white markings each were used in areas A and B in 2007, and in areas C and D in August 2008. In May 2008, time constraints prevented usage of markings.

Georeferencing and rectifying was performed in ArcMap 9.3 (ESRI Inc. 1999-2008). Ancillary map data used for georeferencing included black and white ortophotos, and vector files of hydrology, roads, and buildings from the topographic map at a scale of 1:50 000 (National Land Survey of Sweden). However, the vector files from the topographic map did not match exactly to the ortophotos, due to generalization of roads and rivers in the vector files. Therefore, additional digitizing of hydrological features, roads and houses based on the ortophotos was required for georeferencing of aerial photographs. Rectified images were saved as geotiff. In 2007, all data was handled in RT90 2.5 gonW. In 2008, the new Swedish reference system SWEREF 99TM was used.

For rectifying, first order polynomial transformation was applied for calculation of the root mean square error (RMSE), while "adjust" was used for the final rectifying, with cubic convolution as the resampling method (ESRI Inc. 1999-2008). The polynomial transformation uses a least squares fitting (LSF) algorithm and is optimized for global accuracy but does not guarantee local accuracy. The adjust transformation optimizes for both global LSF and local accuracy by performing a polynomial transformation using two sets of control points and adjusting the control points locally to better match the target control points using a triangulated irregular network (TIN) interpolation technique.

The RMSE (provided in pixels) is a measurement of the accuracy of the transformation and is based on comparing the actual location of the map coordinate to the transformed position in the raster. The distance between these two points is the residual error, and RMSE is computed by taking the root mean square sum of all the residuals.

Edge displacement was evaluated by comparing the rectified images to an ortophoto. The distance (meter) between elements, e.g. roads, ditches, at the edge of the rectified image and the corresponding element on the ortophoto was measured.

2.4 Flood delineation

2.4.1 Ground control points

In August 2008, ground control points for flood delineation were measured using DGPS in areas C and D on the day of the flight. In area C, 75 points were included, and in area D, 58 ground control points were measured. At both locations, water depth (cm) and vegetation height (cm) were recorded for each ground control point. Based on this data, the ground control points were grouped by designating a status with regard to water and vegetation, respectively. All points with water depth = 0 cm were designated water status "dry", and all points with water depth $\geq$ 1 cm were assigned water status "flooded". Regarding vegetation, all points with vegetation height $\leq$ 50 cm were grouped as vegetation status "low" while all points with vegetation > 50 cm were assigned vegetation status "high".

No ground control points for flood delineation were captured in May 2008.

2.4.2 Visual interpretation

Visual interpretation was based on the assumption that the appearance of flooded areas should differ from dry areas, interpreted by human vision. The direct recognition strategy was applied

(Campbell 2005) to identify flooded areas and to differentiate them from adjacent non-flooded areas. The visual interpretability of images was improved by using image enhancements. Enhanced images contain no more information than the original image but enable easier interpretation due to exaggeration of differences in tone and colour (Piwowar 2005). In Arc GIS 9.3, contrast stretching methods were tested, including standard deviation with gamma stretch and histogram equalize.

For further evaluation of the interpretability of images, red-green-blue band values (RGB) were extracted for the ground control points from the August images, using the sample tool and cubic convolution as the resampling technique. The RGB values were tested for correlations with water depth and vegetation height. T-tests were employed to test for differences of band values between grouped points with regard to water status and vegetation status. Statistical evaluation was performed in Statistica (Statistica Inc. 2008).

2.4.3 Unsupervised classification

Unsupervised classification was preferred to supervised classification for two reason: a) to have ground truth information for accuracy assessment, and b) to allow for classification even in locations without further knowledge on flooded areas. Iso Cluster (ArcGIS 9.3) was used as the clustering algorithm. The Iso Cluster tool uses the migrating means algorithm which is the most widely implemented method (Piwowar 2005). The derived cluster statistics were then used as the input for a Maximum Likelihood Classification. This classification assigns each pixel to the class it most likely belongs. According to Piwowar (2005), the Maximum Likelihood Classifications typically produces the most accurate classifications and is thus the preferred method.

The Iso Cluster tool was run with both 10 and 15 classes and with 20 iterations for each image. After the Maximum Likelihood Classification, classes representing flooded and dry areas were chosen, followed by a reclassification resulting in two classes only (flooded and dry). The results (accuracy assessments, see 2.4.5) were compared with regard to differences caused by number of classes (10 or 15) and due to input image format (jpg, full auto processing jpg, 16 bit tiff, full auto processing 16 bit tiff), using t-tests in Statistica (Statistica Inc. 2008).

2.4.4 Digitizing flooded areas

The assumed flooded area was digitized based on the jpg images from August only. The assumed boundary of the flooded area was digitized on screen using the enhanced images and the classified images with 10 and 15 classes, respectively, as the base image.

2.4.5 Accuracy assessment

All unsupervised classifications (both May and August) were evaluated against data based on computations using a digital elevation model (DEM). The DEM is derived from laserscanning with a mean vertical error of less than 20 cm and mean horizontal error of less than 100 cm, and higher accuracy in open than forested environments. For the Norrån system, an elevation value of 56.75 m a.s.l. for the flood in May 2008, and an elevation value of 56.90 m a.s.l for the flood in August 2008 were derived based on GPS measurements (see 2.1) and used as thresholds in a query of the DEM.

Accuracy assessments were performed by using the DEM query result as ground truth for accuracy assessments. An error matrix was obtained by first reclassifying the ground truth raster with dry=1 and flooded=2, and the classification result as dry=10 and flooded=20, followed by summing the grids using raster calculation, using a defined part of the study area as analysis extent (thereby excluding parts of the image with helicopter parts). In the resulting grid, four values were obtained, representing the input values in an error matrix (Table 2.4.1). Based on the error matrix, accuracy assessments including overall accuracy, kappa, producer accuracy, and user accuracy were

computed.

Overall accuracy is defined as the overall proportion of correctly classified pixels The kappa value takes into consideration that the correctly assigned pixels may have been assigned by chance. For example, in a classification with two classes, the random chance that a pixel is classified correctly is 50%. Kappa provides a statistical measure of the agreement between a classification map and a ground-truth map after the chance portion has been accounted for. Producer accuracy indicates the probability that a randomly selected point in the field is correctly classified on the map, while user accuracy refers to the probability that a randomly selected point on the map has the correct class in the field (ground truth). All accuracy assessments were computed following Paine and Kiser (2003).

Table 2.4.1. Values representing the input to an error matrix resulting from addition of reclassified ground truth grid based on data from a digital elevation model and reclassified result of unsupervised classification of aerial photographs.

Classes	Ground truth	
	Dry	flooded
Dry	11	12
Flooded	21	22

The digitized assumed flooded areas were evaluated using the ground control points for areas C and D. Even though this is not comparable to a classification, the resulting boundary was assumed to separate a flooded area from a dry area. Thus, the number of correctly located ground control points could be counted as well as the number of wrongly located points, allowing for an error matrix and calculation of accuracy assessments as described above.

3 Results and Discussion

3.1 Georeferencing

The first flight in April 2007 showed that the white markings were clearly visible from the air and also allowed for easy navigation to the study areas by vision, both from 300 m height (Figure 3.1.1) and 600 m height (Figure 3.1.2). Ditches and forest edges could rather easily be recognized and enabled the orientation of images. Georeferencing and rectifying of images with at least three white markings was very efficient and took approximately 3-5 minutes. Images with less than three or no markings required more information and matching with water courses, ditches, roads and houses.

Displacement at the picture's edge might result in errors. Rectified images taken with wide-angle lens did not show any particular differences to other images, i.e. no increased displacements were observed (Table 3.1.1, Figure 3.1.3).

On May 23, 2007, vegetation had become greener, but the white markings were still visible. Thus, rectifying could be performed in the same way. Unfortunately, no usable image from area A was obtained due to mistakes in focusing. Two images from area B were georeferenced instead. Displacement on these images was rather high, resulting in higher RMSE and high edge displacement on the rectified image (Table 3.1.1).

Table 3.1.1 Summary of georeferencing of aerial photographs from four different flights covering four study areas in the Norrån area close to Österfärnebo, Central Sweden. All images were taken at 600 m height. RMSE is given for 1st order polynomial. Edge displacement was measured in relation to ortophoto. wa=wide angle.

Flight	Helicopter	Images	RMSE	Edge displacement
April 2007	Eurocopter EC120	April07_areaA	8.605	0-28 m
		April07_areaA_wa	5.571	0-6 m
		April07_areaB	4.188	0-18 m
		April07_areaB_wa	5.727	0-4 m
May 2007	Bell 206 Jet	May07_areaB_wa	21.374	5-28 m
	Ranger		6.952	6-27 m
May 2008	Eurocopter EC120	May08_areaB (wa)	4.836	0-9 m
		May08_areaC (wa)	4.050	0-10 m
August 2008	Eurocopter AS 350 B3	Aug08_areaC_1 (wa)	2.920	0-6 m
		Aug08_areaD_1 (wa)	1.501	0-4 m

Figure 3.1.1. Non-georeferenced aerial image over study area B in the Norrån area near Österfärnebo, Central Sweden, with one white marking, flight height 300m, 17 April 2007.

Figure 3.1.2. Non-georeferenced aerial image over study area B in the Norrån area near Österfärnebo, Central Sweden, with three white markings, flight height 600m, 17 April 2007.

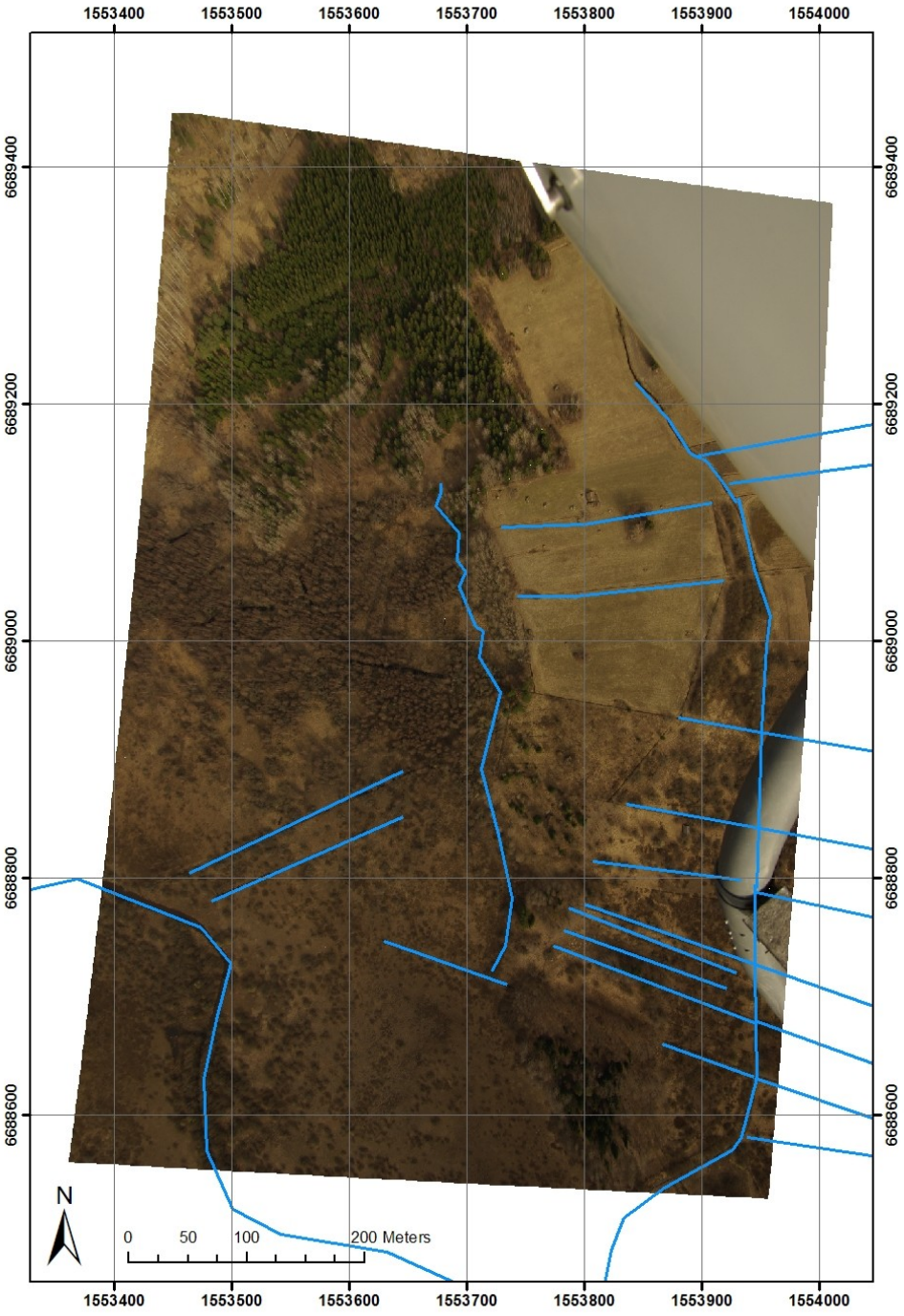

Figure 3.1.3. Rectified image over study area B in the Norrån area near Österfärnebo, Central Sweden, taken on April 2007 from 600 m height and with wide-angle lens (16 mm), including hydrology-information used for rectifying the image.

Georeferencing of images from flights in 2008 was performed both without (May) and with (August) extra white markings. In both cases, the availability of digitized ground information based on an ortophoto allowed for quick and efficient georeferencing.

Comparing helicopter types, best vertical images could be obtained from Eurocopter AS350 B3, flying with open backdoor. The Bell 206 Jet Ranger is least suitable for photographing. It was difficult to find good vertical images, and in addition, parts of the undercarriage showed with varying extent in the centre of the image (Figure 3.1.4). T-tests showed significant differences for

edge displacement between images taken from Eurocopter AS350 B3 and Bell 206 Jet Ranger (t-value=-20.12, df=2, p=0.002), and slightly significant differences for RMSE between images taken from Eurocopter EC120 and Eurocopter AS350 B3 (t-value=-2.55, df=6, p=0.04). Comparison of RMSE and edge displacement between images taken from Eurocopter EC120 and Bell 206 Jet Ranger showed almost significant differences with p=0.05 and p=0.06, respectively.

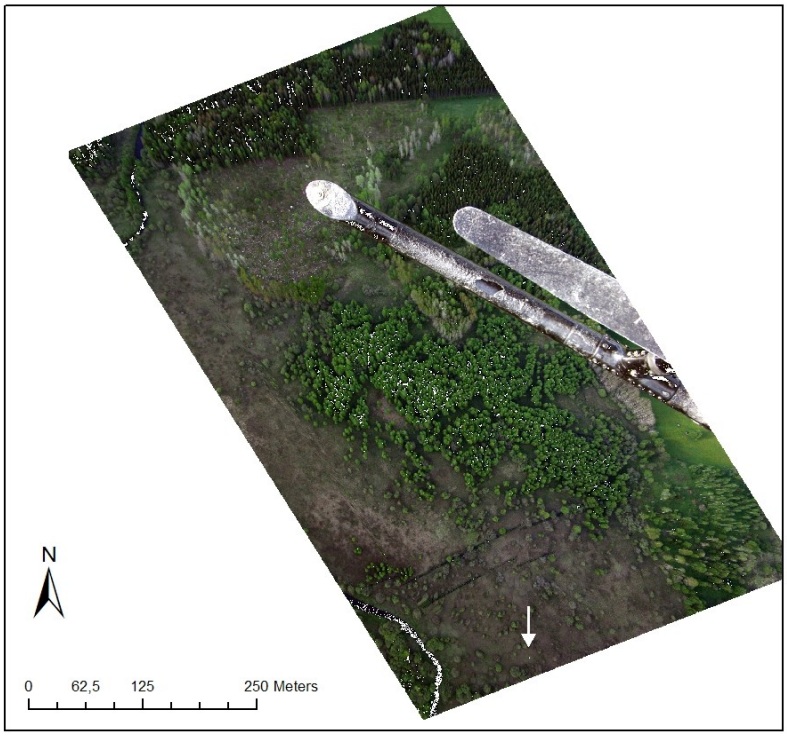

Figure 3.1.4. Rectified image over study area B in the Norrån area near Österfärnebo, Central Sweden, taken in May 2007 from 600 m height and with wide-angle lens.

In summary, I found that using a hand-held digital camera from helicopter gave vertical images of sufficient quality for further use in a GIS. Images obtained at a flight height of 600 m could easily be orientated and georeferenced. At the lower height (300 m), the size covered on ground gets rather small, while at higher heights it gets more difficult to obtain sharp, plane pictures due to increased shaking in the helicopter. Using wide-angle lens increased the coverage of area on ground, thus enabling detection of more ground control points for better georeferencing. The best helicopter type for photographing was the Eurocopter AS 350 B3.

3.2 Flood delineation

3.2.2 Visual interpretation

On all images, direct recognition was possible for the Norrån river due to its shape and its association with trees. Fields could be recognized by their rectangular shape. The potentially flooded areas could be recognized due their site (bordering the river on both sites) and tone. The actual flooded area should be possible to demarcate by its different texture. Areas with surface water were easily distinguished while areas with flooded vegetation (mainly in August) were more difficult to delineate. The interpretability of images was improved by applying image enhancements. Histogram equalizing, as well as standard deviation with gamma stretch (red 0.6, green 0.3 and blue 0.6), made presumingly flooded areas appear darker (Figures 3.2.1 and 3.2.2).

The difference between seasons was very distinct (Figure 3.2.1). On the image from area C in May, dark purple areas correlated to flooded areas and could easily be demarcated. On the image from the same area in August, vegetation had grown dense and complicated recognition of flooded areas, except of the area with surface water. The flooded vegetation did not contrast clearly to non-flooded vegetated areas.

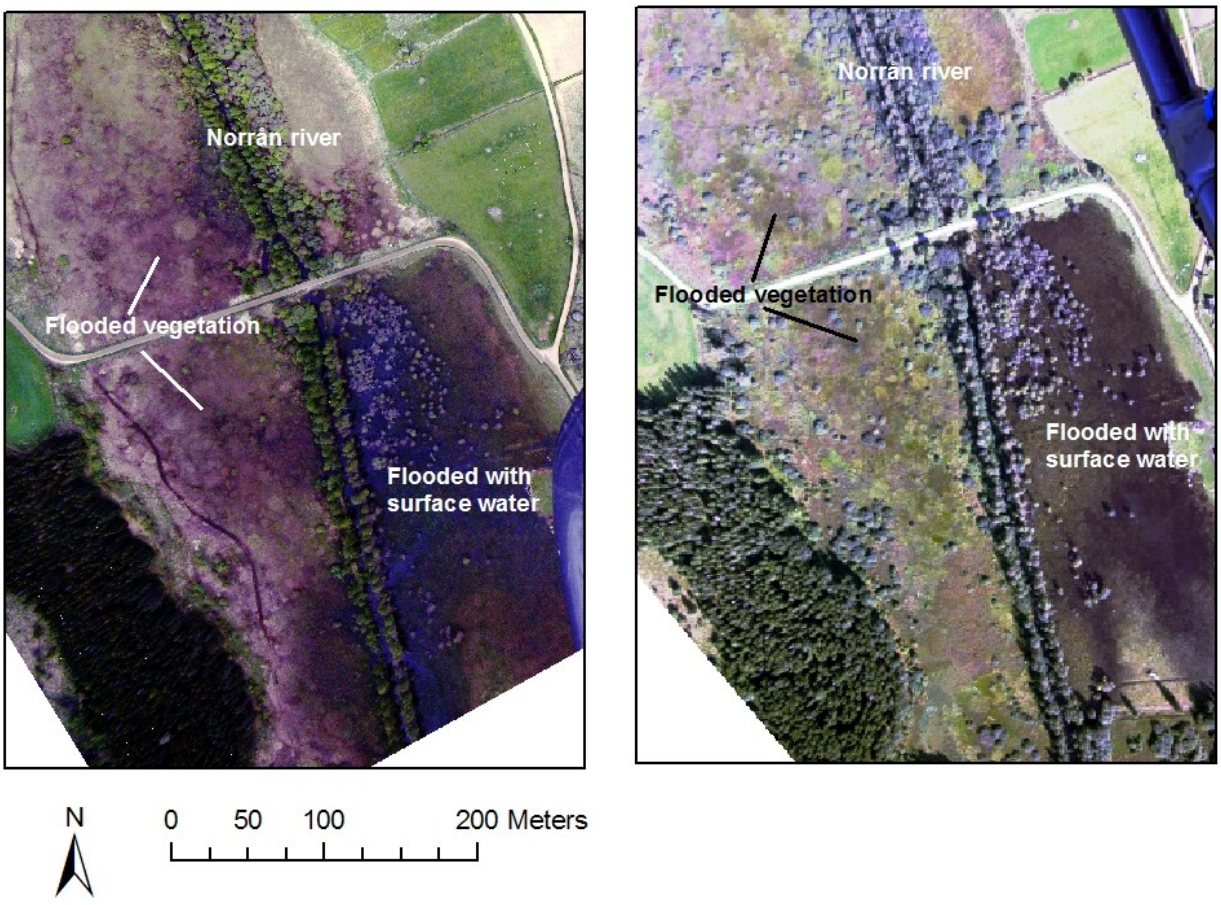

Figure 3.2.1. Visual interpretation of aerial images from study area C in the Norrån area near Österfärnebo, Central Sweden, applying histogram equalization. Left: May 2008; Right: August 2008.

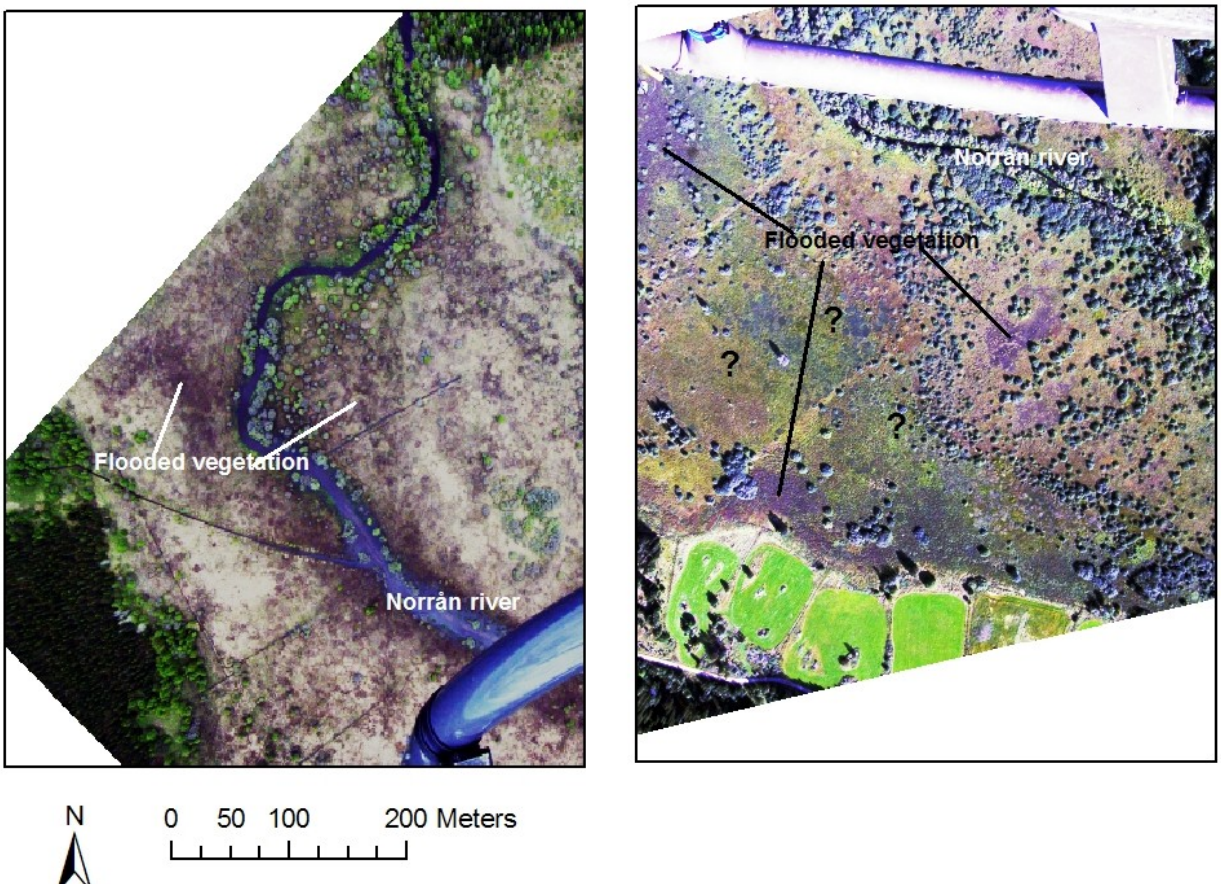

Figure 3.2.2. Visual interpretation of aerial images from study areas B and D in the Norrån area near Österfärnebo, Central Sweden, applying histogram equalization. Left: Area B in May 2008; Right: Area D in August 2008

The effect of dense vegetation also shows in the August image from area D, in comparison with the May image from area B with similar vegetation (Figure 3.2.2). While flooded vegetation could be easily demarcated on the image from area B in May, interpretation of the image from area D in August was difficult. Dark purple areas could relate to flooded vegetation, but there were also large greenish parts separating the purple areas and not clearly recognizable. This reflected the problem in this area with small isolated water puddles caused by rain. Known problems associated with delineation include defining a boundary when there is a transition rather than a sharp edge between two regions (Campbell 2005). The location of the ground control points (Figure 3.2.3) showed this problem in particular in area D where dry and flooded ground control points intermix in a transition zone.

The extracted RGB values of all ground control points (area C and D) from the different image formats showed significant positive correlations between band values and water depth for the red and blue band of image format jpg and the red band of image format full auto processing tiff (Table 3.2.1). The red band of all image formats, as well as the green band of jpg images (format 1 and 2) showed significant negative correlations with vegetation height.

Band values for points grouped as flooded and dry showed no significant differences for any image format. However, histogram equalizing resulted in significant differences for red, green and blue bands of the jpg image, with lower values for dry than for flooded points (t-values red=3.09, green=2.14, blue=1.99, df=84, $p \leq 0.05$; tested for the jpg formats only; Figure 3.2.4). This clearly showed the improvement of the image interpretability by applying image enhancement. Significant

differences for points grouped as high and low vegetation were found for all bands of all image formats with lower band values for points with high than for points with low vegetation.

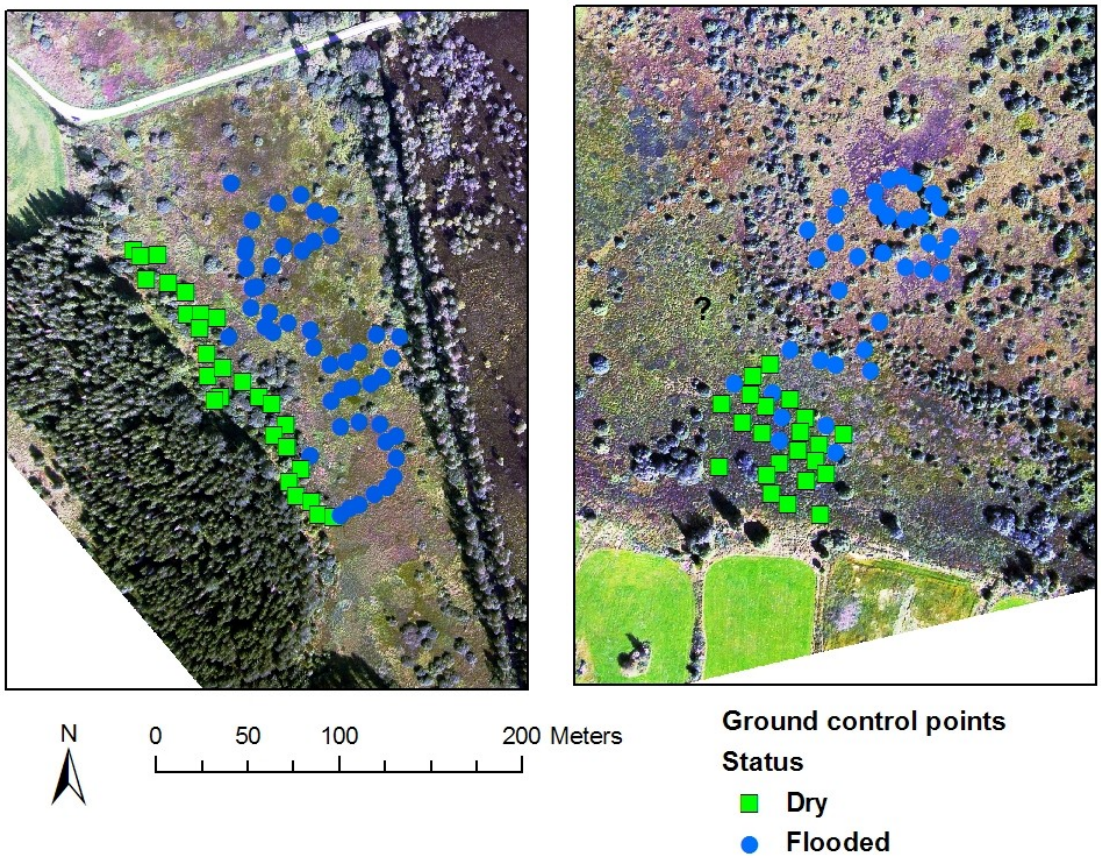

Figure 3.2.3. Location of ground control points measured by GPS from August 2008 in two study areas in the Norrån area close to Österfärnebo, Central Sweden, and grouped as dry (water depth= 0 cm) and flooded (water depth ≥ 1 cm). Left: Area C; right: Area D.

Table 3.2.1. Significant correlations between RGB values of ground control points extracted from aerial images in four different formats covering study areas C and D in the Norrån area close to Österfärnebo, and measured water depth and vegetation height at the locations of the ground control points. All significant correlation $p \leq 0.05$.

Image format	Correlation water depth (Pearson r)	Correlation vegetation height (Pearson r)
1) jpg	Red 0.20 Blue 0.20	Red -0.29 Green -0.21
2) full auto processing jpg	-	Red -0.38 Green -0.28
3) 16 bit tiff	-	Red -0.20
4) full auto processing 16 bit tiff	Red 0.22	Red -0.19

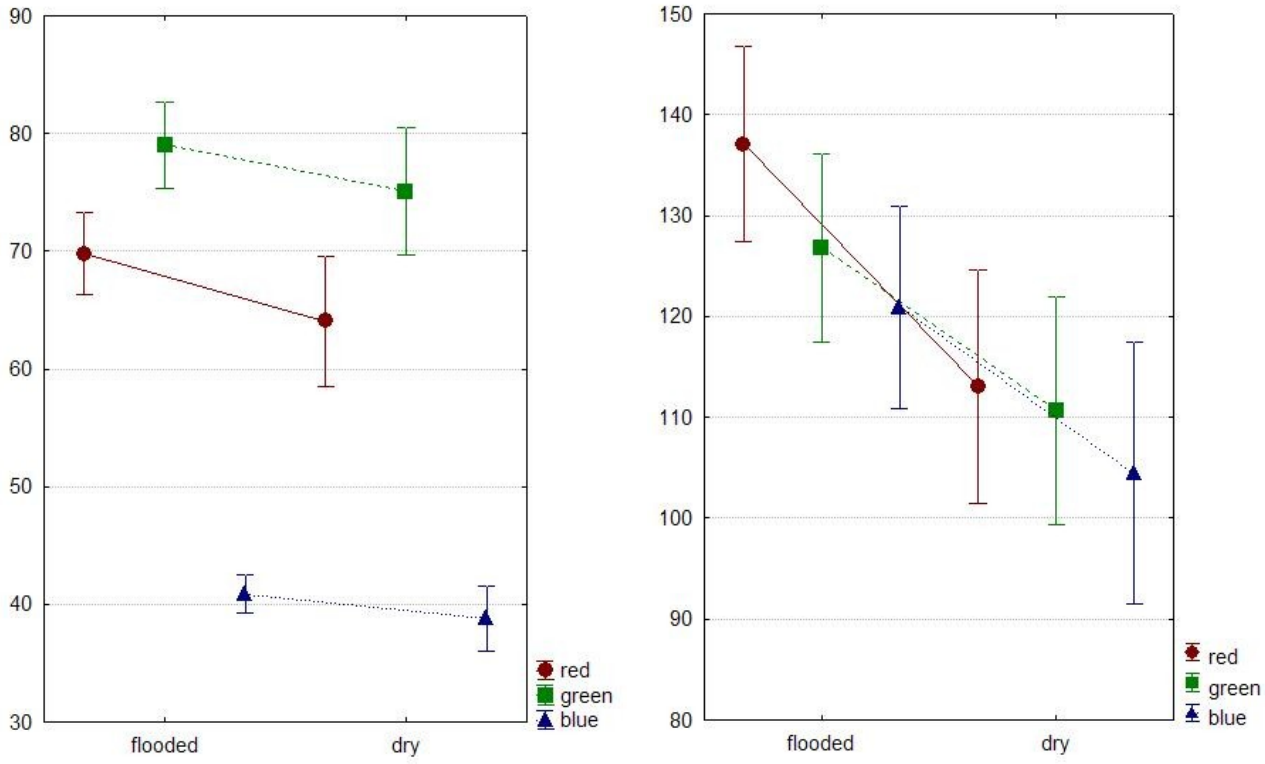

Figure 3.2.4. Mean plot of red, green and blue band values of ground control points grouped as flooded (water depth ≥ 1 cm) and dry (water depth= 0 cm), extracted from aerial images in jpg format over two study areas in the Norrån area near Österfärnebo, Central Sweden. Left: original image; right: after histogram equalizing. Whiskers show 95% confidence interval.

In summary, visual interpretation using image enhancement provided accurate information about location and extent of flooded areas in early summer, but in late summer, vegetated flooded areas might be difficult to differentiate from vegetated non-flooded areas. According to Aronoff (2005), water penetration is provided by blue and green bands. Correlations between band values and water depth were found for the blue and red band, but no significant differences were found between dry and flooded ground control points without image enhancement techniques. However, vegetation might have a bigger impact on values than water depth, which is reflected in correlations of vegetation height and red and green bands. Also, water depth and vegetation height were negatively correlated. Locations with low water and high vegetation were common and most difficult to discern.

More significant statistic results were found for the 8 bit jpg format images (1, 2) than the 16 bit tiff images (3,4), thus it could be concluded that 8 bit images provided sufficient information and 16 bit images did not improve interpretation.

3.2.1 Unsupervised classification

Unsupervised classification showed highest overall accuracy with 75.6 % for classification of the image from May, area C (May_08_areaC), with 15 classes (Table 3.2.2), followed by the classification of the same image with 10 classes (70.1%). These two classifications had also highest Kappa values, indicating that the classification was 48% (15 classes) and 37% (10 classes) better than could be expected by chance alone. Otherwise, good results for overall accuracy (>65%) and Kappa (>0.30) were obtained for classification with 10 classes for all input image formats in area C, and the classification with 15 classes for input format 2 in area C.

According to Skidmore (2002), overall accuracy for land-cover classifications should be at least 85%, but this could not be achieved in this simple classification with dry and flooded areas. He also mentioned that this measure strongly overestimates the positional class accuracy. Other accuracy measurements such as Kappa that takes chance agreement into consideration, provide a better assessment.

When evaluating user and producer accuracy, the practical background of this study implies that producer accuracy for flooded areas is most important. With regard to successful mosquito control operations, it is better to overestimate flooded areas than to underestimate them. Even though an overestimation of flooded areas and thus treatment areas will lead to higher costs for control operations (helicopter, material), an underestimation will lead to increased mosquito emergence and nuisance for the local population.

Highest producer accuracy for flooded areas was obtained for the classification of August image 2 from area C, with 15 classes (87.4%), followed by the May image from area B with 10 classes (80.9%). Producer accuracy between 70 and 80 % were found for the image from May in area C with 15 classes, image 2 from August in Area C with both 10 and 15 classes, and image 2 from august in area D with both 10 and 15 classes.

In most cases, accuracy results were better for images from area C than from area D in August, and better than from area B in May. Also, best results were obtained for the image from May in area C, indicating that detection of flooded areas by unsupervised classification is easier in spring with sparse vegetation than in summer with dense vegetation (compare Figures 3.2.5 and 3.2.6).

Input format

The different image formats tested in August 2008 – 1) jpg, 2) full auto processing jpg, 3) 16 bit tiff, and 4) full auto processing 16 bit tiff – showed in most cases best accuracy results for image 2, full auto processing jpg. The classifications of this image showed consistently higher overall accuracy and kappa than the other input images. The other three input images had rather similar overall accuracy and Kappa values. No significant differences for overall accuracy and kappa between the different input formats were found. Producer accuracy for flooded areas was significantly higher for classifications of images in format 2 than in format 1 (t-value=2.84, df=6, $p<0.05$), format 3 (t-value=3.19, df=6, $p<0.05$), and format 4 (t-value 3.27, df=6, $p<0.05$). Other accuracy assessments did not show significant differences between input formats.

Number of classes

For the images from May, classifications using 15 classes resulted in better accuracy than for classifications using 10 classes, in particular in area C. In area B, producer accuracy for flooded areas was much higher for the classification with 10 classes (80.9%) than with 15 classes (55.9%). Looking at the results for the images from August, classifications with 10 classes had better accuracy results than classifications with 15 classes (both overall accuracy and Kappa). Input image

in format 2, full auto processing jpg, had similar overall accuracy and Kappa for both classifications. A t-test comparing accuracy results for 10 classes and 15 classes (August images only) showed significant higher values for classifications with 10 classes than with 15 classes for overall accuracy (t-value=2.33, df=14, $p<0.05$) and user accuracy for flooded areas (t-value=3.31, df=14, $p<0.05$). Kappa values, user accuracy for dry areas, and producer accuracy for dry areas showed the same trend, whereas producer accuracy for flooded areas had higher mean values for classifications with 15 classes.

Table 3.2.2. Accuracy assessments using DEM queries as ground truth (May: 56.75 m a.s.l.; August: 56.90 m a.s.l) for classifications of aerial images of two study areas in the Norrån area close to Österfärnebo, Central Sweden, taken in May and August 2008 employing 10 and 15 classes.

Images	No classes	Overall accuracy	Kappa	Producer accuracy		User accuracy	
				Flooded	Dry	Flooded	Dry
May08_areaB	10	56.5	0.20	80.9	43.8	42.9	81.5
May08_areaB	15	64.6	0.23	55.9	68.4	44.3	77.6
May08_areaC	10	70.1	0.37	67.2	71.6	55.2	80.8
May08_areaC	15	75.6	0.48	74.2	76.3	62.0	85.1
Aug08_areaC_1	10	65.9	0.31	54.4	76.4	65.9	67.9
Aug08_areaC_2	10	66.7	0.34	79.3	55.1	61.7	74.5
Aug08_areaC_3	10	65.5	0.30	54.4	75.3	66.2	65.1
Aug08_areaC_4	10	65.9	0.31	56.0	75.1	67.5	64.8
Aug08_areaC_1	15	62.0	0.24	65.5	58.8	59.3	65.0
Aug08_areaC_2	15	66.3	0.34	87.4	47.0	60.1	80.3
Aug08_areaC_3	15	61.8	0.24	65.7	58.1	59.7	64.2
Aug08_areaC_4	15	61.8	0.14	55.5	58.7	55.4	58.8
Aug08_areaD_1	10	62.0	0.21	69.0	52.0	67.5	53.7
Aug08_areaD_2	10	62.2	0.20	75.1	43.9	65.5	55.5
Aug08_areaD_3	10	61.6	0.21	66.3	54.9	76.9	53.2
Aug08_areaD_4	10	60.8	0.19	67.8	51.5	65.3	54.3
Aug08_areaD_1	15	57.6	0.11	67.7	43.1	63.2	47.9
Aug08_areaD_2	15	60.7	0.18	70.5	47.0	65.1	53.1
Aug08_areaD_3	15	57.1	0.10	66.6	43.4	62.9	47.5
Aug08_areaD_4	15	57.0	0.10	67.7	42.4	61.3	49.4

Problems with classifications

Evaluation of the results of classifications revealed some problems with this method. Errors in classification were assignment of same class to bushy or forested parts along the river and forests. Fields were often assigned to the same class as open meadows within the flooded wetlands on the August images. When reclassifying, many areas that were included in class "flooded" were therefore located outside the actual area of interest and represented fields or parts of forests.

In summary, the results indicate that applying full auto processing to raw format and saving in jpg format provides the best input image for delineation of flooded areas by unsupervised classification. Regarding the number of classes, 15 classes were preferred for classifications of images from May, while 10 classes gave better results than 15 classes for classification of images from August. An explanation for this pattern could be that the environment in May was still more complex with some green vegetation at some places but not at others (Figure 3.2.5), while in August, vegetation was rather high and homogeneous (Figure 3.2.6), especially in area D (Figure 3.2.7). Thus, more classes resulted in a more accurate classification in May than in August. However, with regard to high producer accuracy of flooded areas, classifications using 15 classes provided better results in particular in area C.

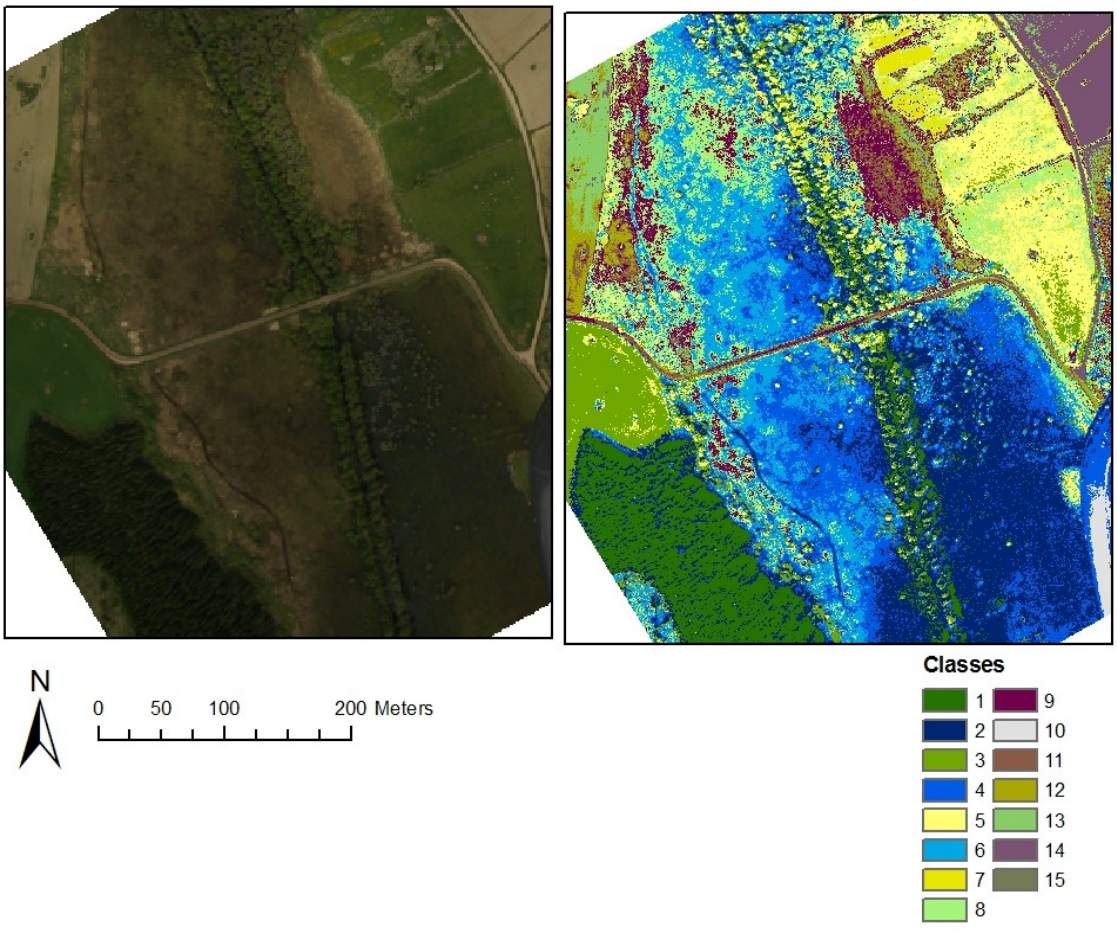

Figure 3.2.5. Unsupervised classification with 15 classes of aerial image of study area C in the Norrån area close to Österfärnebo, Central Sweden, from May 2008 (May08_areaC). left: original image; right: classified image.

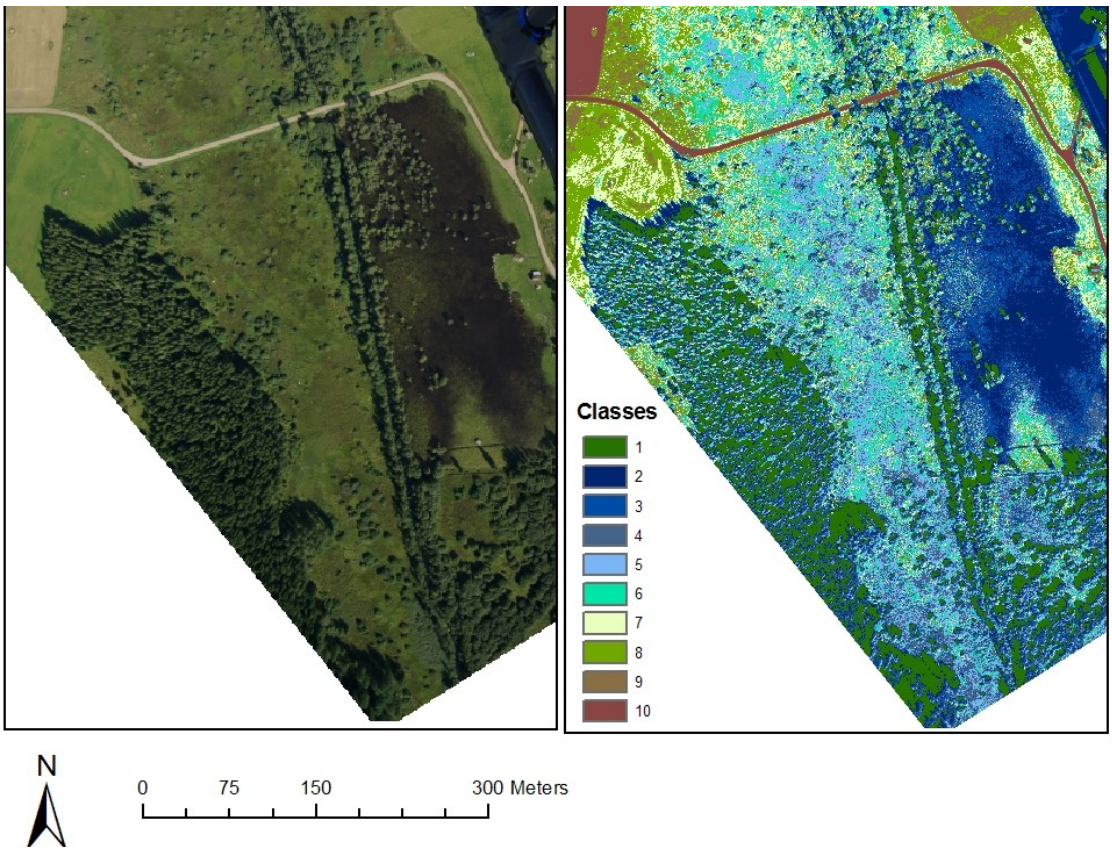

Figure 3.2.6. Unsupervised classification with 10 classes of aerial image of study area C in the Norrån area close to Österfärnebo, Central Sweden, from August 2008 (Aug08_areaC_2). left: Original image; right: Classified image.

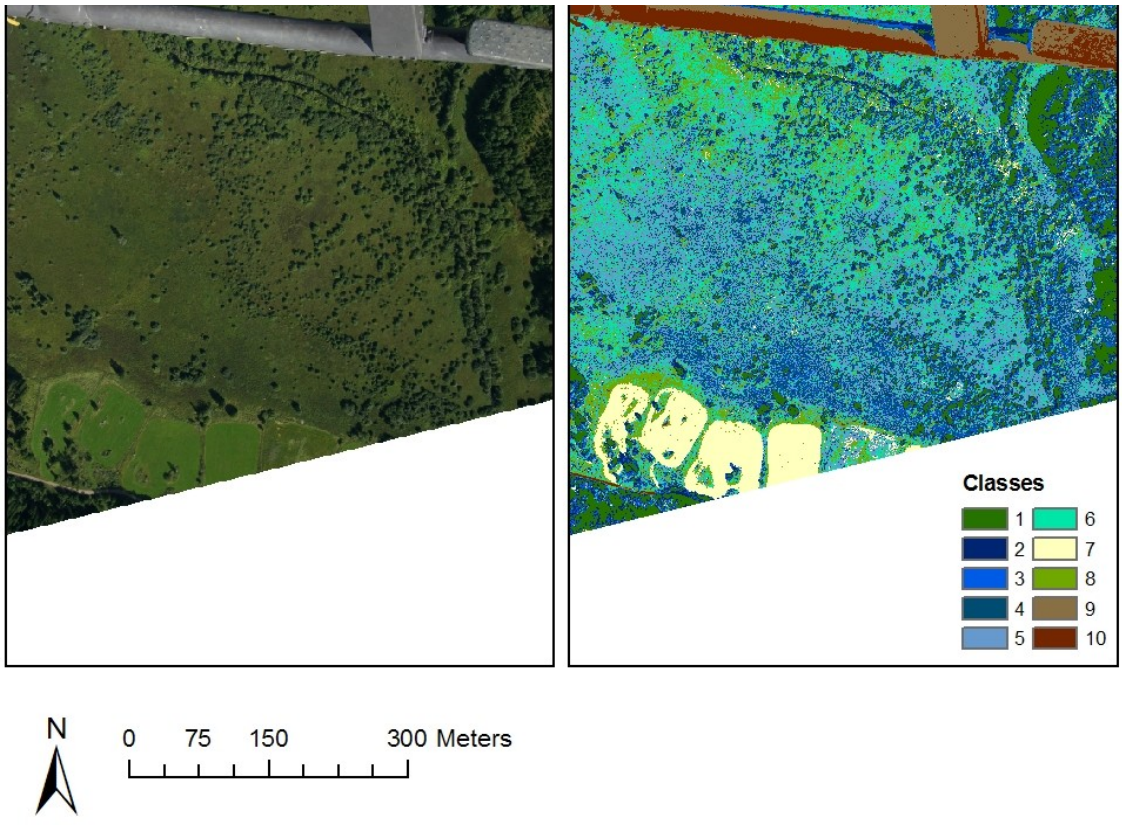

Figure 3.2.7. Unsupervised classification with 10 classes of aerial image of study area D in the Norrån area close to Österfärnebo, Central Sweden, from August 2008 (Aug08_areaD_2). left: original image;right: classified image.

3.2.3 Digitizing flooded areas

The assumed flooded area was digitized based on images 1, jpg, and 2, full auto processing jpg, using the enhanced images (3.2.1) and the classification results (3.2.2) as base images. However, the digitized boundaries from image 1 and 2 were identical, thus only results from image 1 are shown. The results differed largely with regard to the used base image (Table 3.2.3, Figure 3.2.8). Best results were obtained for the boundary based on image enhancements with very high kappa value (0.92) and overall accuracy (96.0 %) for study area C. For study area D, the kappa value indicated that the map was 74% better than expected by chance. Producer accuracy for flooded areas was 100% for the boundaries using classifications as base image, i.e. all flooded ground control points were included in the digitized area (Figure 3.2.8). However, all dry points were included as well in these cases which is reflected in the Kappa values computing to 0.

Table 3.2.3. Accuracy assessments using ground control points as ground truth for digitized assumed flooded areas from aerial images of study areas C and D in the Norrån area close to Österfärnebo, Central Sweden, modified using image enhancement and unsupervised classifications with 10 and 15 classes as base images.

Image	Based on	Overall accuracy	Kappa	Producer accuracy flooded
Aug08_areaC_1	enhanced	96.0	0.92	93.8
Aug08_areaC_1	10 classes	64.0	0.00	100.0
Aug08_areaC_1	15 classes	64.0	0.00	100.0
Aug08_areaD_1	enhanced	87.9	0.74	88.9
Aug08_areaD_1	10 classes	62.1	0.00	100.0
Aug08_areaD_1	15 classes	62.1	0.00	100.0

Including the area actually included in mosquito control treatments showed that the boundary of the mosquito control covered a larger area than any of the digitized boundaries (Figure 3.2.9). Based on the ground control points, the mosquito control area resulted in an overall accuracy of 82.7 % and a kappa of 0.58 in area C, and an overall accuracy of 62.1% and a kappa of 0 in area D. Producer accuracy for flooded areas was 100% for both areas. Most similar to the mosquito control boundaries are the digitized boundaries using classifications as base image.

The larger area of the mosquito control area reflects the consequences of the practical need for generalization. Helicopter flight movements are less time-consuming with straight borderlines, thus the area to be treated might include some small dry parts in order to increase speed and precision of treatments. The pilot covers the exact area by following computer-produced straight flight routes with a specified distance of 16 m (swath width of spreader). A polygon with a complex boundary requires more turns than a polygon with a simplified straight boundary.

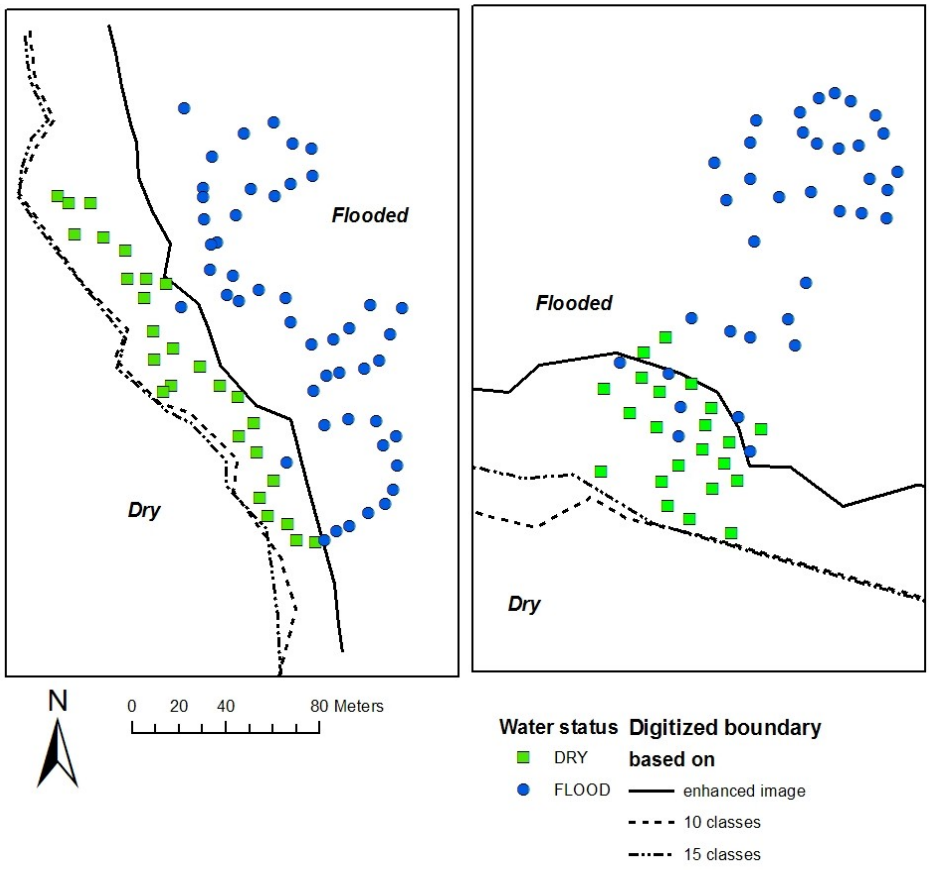

Figure 3.2.8. Digitized boundaries of flooded areas in two study areas in the Norrån area close to Österfärnebo, Central Sweden, in August 2008 in relation to ground control points grouped as dry and flooded. The boundaries are digitized based on aerial images modified using image enhancement and unsupervised classifications with 10 and 15 classes. Left: area C; Right: area D.

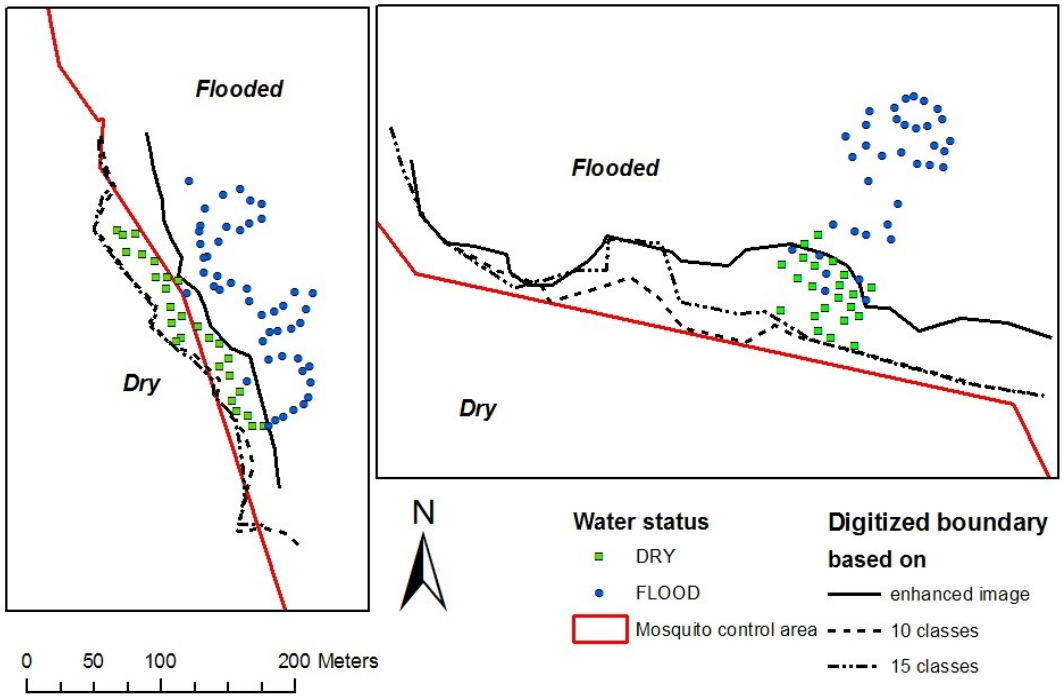

Figure 3.2.9. Digitized boundaries of flooded areas in two study areas in the Norrån area close to Österfärnebo, Central Sweden, in August 2008 in comparison to the actual mosquito control area in August 2008. The boundaries are digitized based on aerial images modified using image enhancement and unsupervised classifications with 10 and 15 classes. Left: area C; Right: area D.

4 Conclusions

The aim of my study was to develop a method for quick and easy delineation of flooded areas to direct mosquito control treatments. Aerial photographs, taken from helicopter using a hand-held digital camera, were georeferenced and used for extracting information about flooded areas in ArcGIS. The methods included image enhancements and unsupervised classifications of aerial images in several input formats and with or without processing in the camera's software.

The results showed that taking photographs in raw format, for further processing in the camera's software, did not improve demarcation of flooded areas, neither did using 16 bit tiff. Thus, this step could be spared and images could be taken in jpg (8 bit) format and imported directly to GIS. Image enhancement with contrast adjustments can be performed in ArcGIS and do not require special camera software.

Both visual interpretation and unsupervised classification showed that it was easier to delineate flooded vegetated areas in spring than in summer. High and dense vegetation in August lead to more homogeneous areas with less marked boundaries. In addition, the flood event in August 2008 was caused by a combination of high water flow in the River Dalälven and local rain, creating both large flooded areas and small isolated water puddles at the edges. Thus, no sharp boundary of the flooded area was formed, complicating delineation both in the field and in the analyses of the aerial images. In this case, a fuzzy classification might have been more appropriate, considering a gradient from 0% flooded to 100% flooded.

Better detection of flooded areas during summer conditions might have been achieved by using the near-infrared (IR) spectrum. Water strongly absorbs near-IR energy which makes this spectrum useful for delineation of water features (Aronoff 2005). The CCD of most digital cameras, including the Pentax 10D, is sensitive to IR but the cameras have an IR blocking filter mounted internally. This blocking filter could be removed, allowing for both visual and IR light to pass. Another option is to use an external filter that allows transmission of IR light. However, according to discussions on the internet (http://photo.net/pentax-camera-forum, http://www.markcassino.com/b2evolution/index.php/cat33), the internal IR blocking filter in the Pentax 10D appears to be very effective and difficult to bypass using an external filter. Also, taking IR pictures with an external filter required very long exposure times. Thus, removing the internal IR blocking filter might be more efficient, but requires more reliable information about the consequences before disassembling the camera.

For directing helicopter-based mosquito control, digitized polygons of the areas for treatment are needed. Using enhanced aerial images as the base image for digitizing treatment areas resulted in best accuracy evaluated with ground control points. However, based on the results of unsupervised classifications, the digitized boundaries were more similar to the actual mosquito control area. For practical reasons, it is acceptable to include small dry parts in treatments areas. From this aspect, the best method appears to be unsupervised classification of a jpg-image, and on-screen digitizing of the boundaries of flooded areas. Manually mapping boundaries include the difficulty that the decision where to draw the boundary is partly subjective (Brown and Young 2006), and thus might differ between individuals. This should be tested and in case several people are involved in preparing treatment areas, training should be provided to ensure similar results in digitized boundaries.

This rather simple approach has the advantage that it does not require expensive commercial software. Georeferencing, unsupervised classification and on-screen digitizing can be performed in open source GIS software such as GRASS and Quantum GIS. In a test, I used Quantum GIS and GRASS and could accomplish georeferencing, unsupervised classification and on-screen digitizing with very good results.

The suggested method for near real-time mapping of floodwater mosquito breeding sites using

aerial photographs needs to be further tested under time constraints during mosquito control activities. In 2009, photographs were taken over an inaccessible area and after georeferencing compared to the suggested treatment area (based on digital elevation model) using image enhancement. This resulted in a slightly enlarged treatment area. Thus, the method offers possibility to adjust and improve the delineation of flooded areas for mosquito control.

5 Acknowledgements

I want to thank my supervisor at Lund University, Ulrik Mårtensson, for his support and all help and comments. I also want to take the opportunity to thank all teachers at LUMA GIS for doing a great job, I enjoyed my studies a lot!!

Jan Lundström supported my idea to study GIS, and practically helped with GPS measurements in the field and comments on this thesis. Thanks a lot for your continuous support, let's see what comes next!

Thanks also to the skilful helicopter pilots at Osterman Helicopter AB who participated in this: Franklin Eck, Michael Elmeskog, Dennis Sundquist, Bengt-Inge Thagg, and Lars Åsengård.

6 References

Aronoff, S. 2005. Remote sensing basics, pp. 197-244. *In* S. Aronoff [ed.], Remote Sensing for GIS Managers. ESRI Press, Redlands, California.

Becker, N., D. Petric, M. Zgomba, C. Boase, C. Dahl, J. Lane and A. Kaiser. 2003. Mosquitoes and their control. Kluwer Academic/Plenum Publishers, New York, USA.

Brown, L. and K.L. Young. 2006. Assessment of three mapping techniques to delineate lakes and ponds in a Canadian High Arctic wetland complex. Arctic 59: 283-293.

Brust, R.A. 1980. Dispersal behavior of adult *Aedes sticticus* and *Aedes vexans* (Diptera: Culicidae) in Manitoba. The Canadian Entomologist 112: 31-42.

Campbell, J.B. 2005. Visual interpretation of aerial imagery, pp. 259-285. *In* S. Aronoff [ed.], Remote sensing for GIS managers. ESRI Press, Redlands, California.

Falkner, E. and D. Morgan. 2002. Aerial mapping methods and applications. CRC Press, Boca Raton, FL.

Paine, D.P. and J.D. Kiser. 2003. Aerial photography and image interpretation. John Wiley & Sons, Hoboken, NJ

Piwowar, J.M. 2005. Digital image analysis, pp. 287-335. *In* S. Aronoff [ed.], Remote sensing for GIS managers. ESRI Press, Redlands, California.

Schäfer, M. and J.O. Lundström. 2006. Mygg-GIS. Sinus 3: 4-6.

Schäfer, M.L., J.O. Lundström and E. Petersson. 2008. Comparison of mosquitoe (Diptera: Culicidae) populations by wetlands type and year in the lower River Dalälven region, Central Sweden. J. Vector. Ecol. 33: 150-157.

Schäfer, M.L. and J.O. Lundström. 2009. The present distribution and predicted geographic expansion of the floodwater mosquito *Aedes sticticus* in Sweden. J. Vector. Ecol. 34: 141-147.

Skidmore, A.K. 2002. Accuracy assessment of spatial information, pp. 197-209. In A. Stein, F.v.d. Meer and B. Gorte [eds.], Spatial Statistics for Remote Sensing. Kluwer Academic Publishers, The Netherlands.

Statistica Inc. 2008. STATISTICA (data analysis software system) computer program, version version 8.0. StatSoft Inc.,Tulsa, USA.

Internet references

http://extoxnet.orst.edu/pips/bacillus.htm. Extoxnet, Extension Toxicology Network, Pesticide Information Profiles: Bacillus thuringiensis. Revised June 96. Latest visit September 2009.

http://photo.net/pentax-camera-forum\. Photo.net. A community of photographers. Pentax forum. Latest visit March 2010.

http://www.markcassino.com/b2evolution/index.php/cat33/ CalArti. A photographer's journal. Category: Pentax K10D. Digital infrared with the Pentax K10, March 16, 2007. Latest visit March 2010.

Series from Lund University's Geographical Department

Master Thesis in Geographical Information Science (LUMA-GIS)

1. *Anthony Lawther:* The application of GIS-based binary logistic regression for slope failure susceptibility mapping in the Western Grampian Mountains, Scotland. (2008).
2. *Rickard Hansen:* Daily mobility in Grenoble Metropolitan Region, France. Applied GIS methods in time geographical research. (2008).
3. *Emil Bayramov:* Environmental monitoring of bio-restoration activities using GIS and Remote Sensing. (2009).
4. *Rafael Villarreal Pacheco:* Applications of Geographic Information Systems as an analytical and visualization tool for mass real estate valuation: a case study of Fontibon District, Bogota, Columbia. (2009).
5. *Siri Oestreich Waage:* a case study of route solving for oversized transport: The use of GIS functionalities in transport of transformers, as part of maintaining a reliable power infrastructure (2010).
6. *Edgar Pimiento:* Shallow landslide susceptibility – Modelling and validation (2010).
7. *Martina Schäfer:* Near real-time mapping of floodwater mosquito breeding sites using aerial photographs (2010)